

**Table I.** Optically Active Polymers of  $\text{CH}_2=\text{C}(\text{CH}_3)\text{CO}_2\text{R}$  Produced with Chiral Host Initiators at  $-78^\circ\text{C}$  in 95% Toluene-5% THF, 95-100% Conversion

run no.	R of ester	catalyst	[ester]/[catalyst]	tacticity, % <sup>a</sup>			$\bar{M}_n^b$ (D)	$[\alpha]^{25}_{578}$ (THF, c 2)	
				iso	syn	het		initial <sup>c</sup>	later, h
1	Me	(S)-1-KO- <i>t</i> -Bu	5	80	5	15	480 (1.06)	+250°	+40° (5)
2 <sup>d</sup>	Me	(S)-1-KO- <i>t</i> -Bu	15	78	2	20	1600 (1.2)	+248°	+20° (5)
3	Me	(S,S)-2-KO- <i>t</i> -Bu	100	88	7	5	<i>e</i>	-180°	<i>e</i>
4 <sup>f</sup>	Me	(S,S)-3-LiBu	10	90	2	8	1100 (1.1)	+70°	+10° (24)
5	<i>t</i> -Bu	(S)-1-KO- <i>t</i> -Bu	11	90	5	5	1600 (1.3)	+117°	+78 (18) +2° (42)
6	<i>t</i> -Bu	(R)-1-KO- <i>t</i> -Bu	30	90	7	3	<i>e</i>	-150°	<i>e</i>
7	PhCH <sub>2</sub>	(S)-1-KO- <i>t</i> -Bu	12	not	determ		2100 (1.5)	+350°	no change

<sup>a</sup> Determined from <sup>1</sup>H NMR methyl chemical shifts in polymer backbone; isotactic,  $\delta$ , 1.24; syndiotactic, 0.85; heterotactic, 1.09. The spectra were consistent with  $\text{I}-[\text{CH}_2\text{C}(\text{CH}_3)(\text{CO}_2\text{R})]_n\text{-H}$  structures. <sup>b</sup>  $\bar{M}_n$  and  $\bar{M}_w$  determined by GPC; polydispersity,  $D = \bar{M}_w/\bar{M}_n$ . <sup>c</sup> Taken after about 5 h or less handling time at ambient temperature. <sup>d</sup> The procedure is illustrated. To a dry solution of 0.56 g of KO-*t*-Bu and 2.58 g of (S)-1 in 1 mL of THF stirred under Ar was added 19 mL of toluene, followed by 7.50 g of  $\text{CH}_2=\text{C}(\text{CH}_3)\text{CO}_2\text{CH}_3$  (dropwise,  $-78^\circ\text{C}$ , 15 min, syringe pump). The mixture was stirred at  $-78^\circ\text{C}$  for 3 h, 3 mL of  $\text{CH}_3\text{OH}$  was added, the solvent was evaporated under vacuum, and the product was purified by preparative GPC (Styragel-THF) and preparative HPLC (silica gel, EtOAc-BuCl, 1:1 by volume). <sup>e</sup> Not taken. <sup>f</sup> Run in pure toluene.

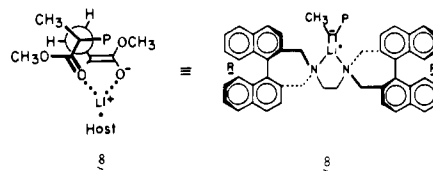
special example of the Michael addition reaction, we anticipated that 1-3 complexed with metal bases would act as chiral catalysts to "stamp out" asymmetric units to give optically active isotactic polymers. The carbanion ion paired to the host-bound cation is present at the growing end of the chain. Thus, any configurational "mistake" would tend to be corrected rather than perpetuated in the successive generation of asymmetric centers.<sup>4</sup> After we had observed high rotations for our methyl methacrylate polymer, Yuki et al. reported that (-)-sparteine-BuLi-initiated polymerization of trityl methacrylate gave optically stable isotactic polymer whose high optical rotation was attributed to helicity.<sup>5</sup> The only other known synthetic polymers that are helically chiral are the poly(alkyl isocyanides), which show high configurational stability.<sup>6</sup>

Table I illustrates our results. Runs not recorded here established that for each of the three catalysts, inverting the configurations of the catalysts inverted the signs of rotation of the polymer produced, as is illustrated in runs 5 and 6. When the *tert*-butyl polyester from run 5 ( $[\alpha]^{25}_{578} +117^\circ$ ) was cleaved in methanolic HCl under mild conditions, and the polyacid produced was treated with  $\text{CH}_2\text{N}_2$ , the methyl polyester obtained gave  $[\alpha]^{25}_{578} +2^\circ$ . The chromatographic and <sup>1</sup>H NMR properties of the polymers showed the absence of byproducts that often accompany anionic polymerization.<sup>7</sup>

The results indicate that all three catalysts with methyl, *tert*-butyl, or benzyl methacrylate gave highly isotactic polymers with high optical rotations whose sign depended on the configuration of the catalyst and was independent of the nature of the R group of the ester monomer. More interestingly, the polymers with methyl and *tert*-butyl ester groups mutarotated at ambient temperature over a period of hours to give rotations close to zero, whereas the polymer with the benzyl ester group was optically stable over similar time spans. We conclude that the high rotations are due to helicity of the polymers induced by the chiral cavities of the catalyst in which each unit is added to the growing chain. The helices of at least the methyl and *tert*-butyl ester polymers appear to be thermodynamically unstable kinetic products of the polymerization, whose conformations randomize over a period of hours to give a small residual optical rotation associated with the mesolike interior and different end groups of isotactic polymer (i.e., 4 produced in run 1). We do not understand why the benzyl ester helix is more stable than the *tert*-butyl ester helix. As expected, the polyacid derived from the optically active *tert*-butyl ester polymer randomized before it could be reesterified.

The patterns of relationships between the configurations of the catalysts employed and the signs of rotations of the helical

polymers produced are coherent with the patterns observed for the simple Michael reactions. Thus, (S)-1-KOBu-*t* always gave (+) polymer and (S,S)-2-KOBu-*t* gave (-) polymer. These two catalysts provided opposite chiral biases in the Michael additions as well.<sup>2</sup> Similar stereoelectronic factors probably operate in both the Michael additions and polymerizations. Structures 5, 7, and 8 are suggested models for the dominant transition states for the



carbon-carbon bond-forming steps of the propagation reactions. These models account for the facts, predict the configurations of the asymmetric centers of the polymers, and predict the helical configurations as well. Thus, 5 and 8 predict helical polymer 6 with a counterclockwise helix, while 6 predicts an enantiomeric polymer with a clockwise configuration. The mechanism of the conformational randomization of helical isotactic poly(methyl methacrylate) presents an interesting problem potentially amenable to a computational modeling.

### Electronic Conductivity of Poly[tris(5,5'-bis[(3-acrylyl-1-propoxy)carbonyl]-2,2'-bipyridine)ruthenium(0)]

C. Michael Elliott,\* J. G. Redepenning,<sup>†</sup> and Ethan M. Balk<sup>‡</sup>

Department of Chemistry, Colorado State University  
Fort Collins, Colorado 80523  
Received September 6, 1985

We have previously reported electrochemical and spectral studies of electrodes modified with polymer films (poly-1) prepared from the monomeric complex  $\text{RuL}_3^{+2}$  (1) where  $\text{L} = 5,5'$ -bis-[(3-acrylyl-1-propoxy)carbonyl]-2,2'-bipyridine.<sup>1,2</sup> These films are electroactive having seven stable oxidation states (2+ to 4-).<sup>2</sup> Here we report that, under certain solution and potential conditions, poly-1 in its zero formal oxidation state is an electronic conductor having specific conductivities approaching those reported for doped polyquinoline.<sup>3</sup> By employing a soluble cationic polymer as the supporting electrolyte, negative formal oxidation states of poly-1 are prevented from forming by the selective steric exclusion of cations. By thus locking poly-1 into a single oxidation state it is possible to measure its electronic conductivity without the

(4) (a) Cram, D. J.; Kopecky, K. R. *J. Am. Chem. Soc.* **1959**, *81*, 2748-2762. (b) Cram, D. J.; Wilson, D. R. *J. Am. Chem. Soc.* **1963**, *85*, 1249-1257.

(5) Okamoto, Y.; Suzuki, K.; Ohta, K.; Hatada, K.; Yuki, H. *J. Am. Chem. Soc.* **1979**, *101*, 4763-4765.

(6) (a) Nolte, R. J. M.; van Beijnen, A. J. M.; Drenth, W. *J. Am. Chem. Soc.* **1974**, *96*, 5932-5933. (b) Drenth, W.; Nolte, R. J. M. *Acc. Chem. Res.* **1979**, *12*, 30-35.

(7) See, for example: Piejko, K.-I.; Höcker, H. *Macromol. Chem. Rapid Commun.* **1982**, *3*, 243-247 and references therein.

<sup>†</sup> Present address: California Institute of Technology.

<sup>‡</sup> Present address: Williams College, Williamstown, MA.

(1) Elliott, C. M.; Hershenhart, E. J. *J. Am. Chem. Soc.* **1982**, *104*, 7519.

(2) Elliott, C. M.; Redepenning, J. G. *J. Electroanal. Chem.*, in press.

(3) Tunney, S. F.; Suenaga, J.; Stille, J. K. *Macromolecules* **1983**, *16*, 1398.

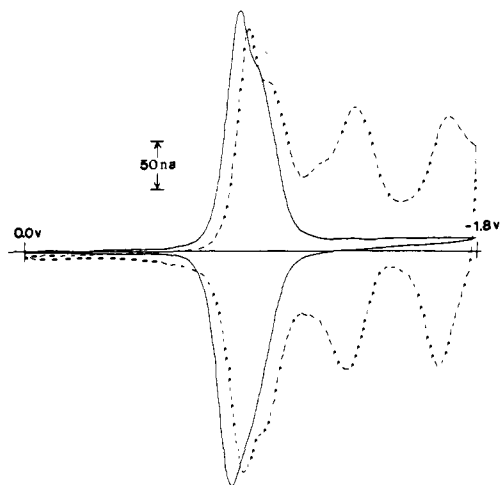


**Figure 1.** Cyclic voltammograms of a 0.25-mm-diameter platinum electrode modified with an  $\sim 1.0\text{-}\mu\text{m}$  film of poly-1. Scan rate = 50 mV/s. Volts vs. Ag/Ag<sup>+</sup> (0.10 M in Me<sub>2</sub>SO) reference. (—) 0.10 M PDDP polymer electrolyte in acetonitrile. (---) 0.10 M TBA<sup>+</sup>PF<sub>6</sub><sup>-</sup> electrolyte in acetonitrile.

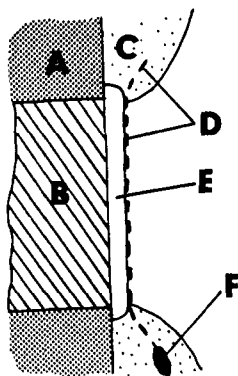


**Figure 2.** Schematic representation of a cross section of the "sandwich" electrode used for conductivity measurements of poly-1. (A) Pyrex mount, (B) glassy carbon electrode, (C) epoxy mask, (D) porous gold minigrad electrode, (E) poly-1 film, (F) silver paint contact for Au electrode. The figure is not drawn to scale; e.g., the relative polymer thickness has been greatly exaggerated.

complications of any concomitant redox conduction (as could be the case with a conventional electrolyte).

Figure 1 shows cyclic voltammograms (CV) of a platinum electrode coated with an  $\sim 1\text{-}\mu\text{m}$ -thick film of poly-1. The dashed curve is the CV in a standard electrolyte (0.10 M TBA<sup>+</sup>PF<sub>6</sub><sup>-</sup>); the solid curve is for an identical electrode but employing 0.10 M poly(1,1-dimethyl-3,5-dimethylenepiperidinium hexafluorophosphate) (PDDP) as the electrolyte. In both electrolytes the first two redox processes (2<sup>+</sup>/1<sup>+</sup> and 1<sup>+</sup>/0), involving counteranions, are present at approximately the same potential. The more negative reductions are absent for the PDDP electrolyte, ostensibly due to the inability of the polycation to enter the poly-1 film.

The conductivity of the polymer as a function of oxidation state was monitored by using a "sandwich" electrode similar in concept to that reported by Murray and co-workers<sup>4</sup> and constructed in the manner shown in Figure 2. A relatively thick film of 1 was first deposited on a planar glassy carbon electrode (GC) and thermally polymerized (150 °C, 12 h). A second very thin film ( $\ll 1\ \mu\text{m}$ ) of 1 was then spin-coated over the first film and a piece of Au minigrad was pressed onto the surface. The assembly was heat-treated a second time (150 °C, 12 h) to bond the Au to the poly-1 surface. Electrical contact was provided to the edge of gold electrode using a conducting silver paint. Finally, the

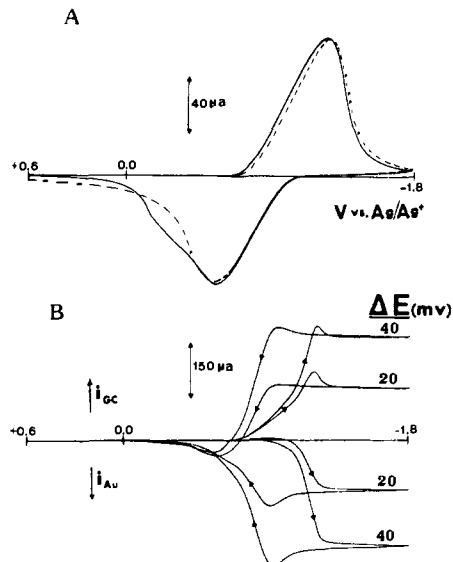


**Figure 3.** (A) Cyclic voltammograms obtained on a 3.7- $\mu\text{m}$ -thick polymer "sandwich" electrode in acetonitrile 0.10 M PDDP. Volts vs. Ag/Ag<sup>+</sup> (0.10 M in Me<sub>2</sub>SO) reference. Scan rate = 50 mV/s. (—) Obtained on the GC electrode with the Au at open circuit, (---) obtained on the Au electrode with the GC at open circuit. (B) Same conditions as above while controlling the potential of both the Au and GC electrodes such that a small constant difference in potential,  $\Delta E = E_{\text{Au}} - E_{\text{GC}}$ , was maintained between the two electrodes.

GC/polymer/Au was masked with epoxy so as to expose only the Au surface to solution.

When the electrode was exposed to a 0.10 M solution of PDDP in acetonitrile, the resistance measured between the Au and GC electrodes (digital ohm meter) was  $>15\ \text{M}\Omega$ . A standard four-electrode potentiostat (Pine Instruments Model RDE 3) was used to measure the film resistance under potential control. The potential of each electrode (i.e., GC and Au) could thus be controlled independently relative to an isolated Ag/Ag<sup>+</sup> (0.10 M in Me<sub>2</sub>SO) reference ( $\sim +0.2\ \text{V}$  vs. SCE). Initially, the potential of each electrode was scanned independently while the other electrode was maintained at open circuit (three-electrode configuration). The CV's obtained are shown in Figure 3A. The broad and featureless shapes of the  $i$  vs.  $E$  curves are typical of those obtained for very thick and/or highly cross-linked films (due to the double thermal polymerization).

To measure the cell resistance the four-electrode configuration was employed.<sup>4</sup> The two electrodes (Au and GC) were simultaneously scanned in the negative direction while a small potential difference (0–40 mV) was maintained between them. The current response is shown in Figure 3B. Over the potential range positive of the foot of the reduction wave, the film resistance remained virtually infinite; consequently no current flowed. Upon reaching the potential where the reduction of the film occurred, the resistance of the polymer dropped. At potentials sufficiently negative to produce the zero oxidation state film, a steady-state value of 120  $\Omega$  was reached. This resistance value, calculated from the current and the applied  $\Delta E$ , agreed closely with the value obtained with a conventional digital ohm meter (109  $\Omega$ ). From the approximate solution-exposed geometric area (0.06 cm<sup>2</sup>) and the microscopically determined unswollen polymer thickness (3.7  $\mu\text{m}$ ), an upper limit to specific resistance of  $<1.9 \times 10^4\ \Omega\ \text{cm}$  is obtained for the reduced film.<sup>5</sup>

The  $i$  vs.  $E$  curves (Figure 3B) generally track the features in CV of the film (Figure 3A). The hysteresis in the  $i$  vs.  $E$  curves

(4) Pickup, P.; Kutner, W.; Leidner, C. R.; Murray, R. W. *J. Am. Chem. Soc.* 1984, 106, 1991.

(5) The facts that (1) the degree of polymer swelling is unknown, (2) the spacings of the grid in the Au electrode are large relative to the polymer thickness (1000 lines/in.,  $\sim 21 \times 21\ \mu\text{m}$  hole size), and (3) the actual area of contact between the Au and poly-1 surface is unknown make it impossible to calculate an exact specific resistance. In fact, the value of  $1.9 \times 10^4\ \Omega\ \text{cm}$  may overestimate the actual specific resistance by more than an order of magnitude and almost certainly by at least a factor of X4.

in Figure 3B is due to the fact that in this experiment the faradaic current from the redox chemistry of the poly-1 film is superimposed on the ohmic current between the Au and GC electrodes. This can be demonstrated by plotting  $i_{GC} + i_{Au}$  vs.  $E_{Au}$  (for small  $\Delta E$ ) which nearly quantitatively reproduces the CV of the polymer (i.e., Figure 3A). The potential offsets between the positive and negative scans, respectively, match up well with the peak currents for the CV and thus are attributable to the slow response of the thick, highly cross-linked polymer film used to obtain Figure 3. Once the steady state is reached, however,  $-i_{Au} = i_{GC}$  within experimental error.<sup>6</sup>

While the specific resistance of reduced poly-1 is significantly larger than those of many other organic electronic conductors,<sup>7-13</sup> it does approach that of many semiconductors. The fact that the electronic conductivity is as large as it is unusual, considering that (1) poly-1 is, by X-ray diffraction, amorphous, (2) it lacks any long-range conjugation, and (3) the redox sites are all, within experimental error, in a single oxidation state. Detailed studies of this behavior are presently under further investigation.

(6) It should be noted here that, because of the use of the polymer electrolyte PDDP, at potentials negative of  $\sim -1.00$  V (cf. Figure 1) only a single oxidation state of poly-1 (i.e., zero) is accessible by either electrode. Thus the mode of conduction between the electrodes cannot be due to redox conduction (an oxidation state concentration gradient).

(7) Shacklette, L. W.; Chance, R. R.; Ivory, D. M.; Miller, G. G.; Baughman, R. H. *Synth. Met.* **1979**, *1*, 307.

(8) Shiradawa, H.; Louis, E. J.; MacDiarmid, A. G.; Chiang, C. K.; Heeger, A. J. *J. Chem. Soc., Chem. Commun.* **1977**, 578.

(9) Rabolt, J. R.; Clarke, T. C.; Kanazawa, K. K.; Reynolds, J. R.; Street, G. B. *J. Chem. Soc., Chem. Commun.* **1980**, 347.

(10) Chance, R. R.; Shacklette, L. W.; Miller, G. G.; Ivory, D. M.; Sowa, J. M.; Eisenbaumer, R. L.; Baughman, R. H. *J. Chem. Soc., Chem. Commun.* **1980**, 348.

(11) Perlstein, J. *Angew. Chem., Int. Ed. Engl.* **1977**, *16*, 519.

(12) Schramm, C. J.; Scaringe, R. P.; Stojakovic, D. R.; Hoffman, B. M.; Ibers, J. A.; Marks, T. J. *J. Am. Chem. Soc.* **1980**, *102*, 6702.

(13) Kanazawa, K. K.; Diaz, A. F.; Greiss, R. H.; Gill, W. D.; Kwak, J. F.; Logan, J. A.; Rabolt, J. F.; Street, G. B. *J. Chem. Soc., Chem. Commun.* **1979**, 854.

## N-Carboxybiotin Formation by Pyruvate Carboxylase: The Stereochemical Consequence at Phosphorus

David E. Hansen and Jeremy R. Knowles\*

Department of Chemistry, Harvard University  
Cambridge, Massachusetts 02138

Received August 16, 1985

The mechanism of the ATP-dependent enzyme-catalyzed reaction of bicarbonate with biotin to give  $N_1$ -carboxybiotin, ADP, and  $P_i$  has been debated since the critical observation of Boyer and co-workers in 1962 that when  $HC^{18}O_3^-$  is used as the substrate for propionyl-CoA carboxylase in unlabeled water,  $^{18}O$  is incorporated into the products methylmalonyl-CoA and  $P_i$  in the ratio of 2:1.<sup>1</sup> This result, along with the large amount of mechanistic data that has subsequently been published on the six enzymes<sup>2</sup> that catalyze the ATP-dependent carboxylation reaction,<sup>3</sup> has led to the three favored pathways shown in Figure 1. In mechanism 1 ("stepwise"), ATP reacts with bicarbonate to form the reactive mixed anhydride carboxy phosphate, which is then attacked by the apparently nonnucleophilic<sup>4</sup> ureido  $N_1$  nitrogen atom of biotin

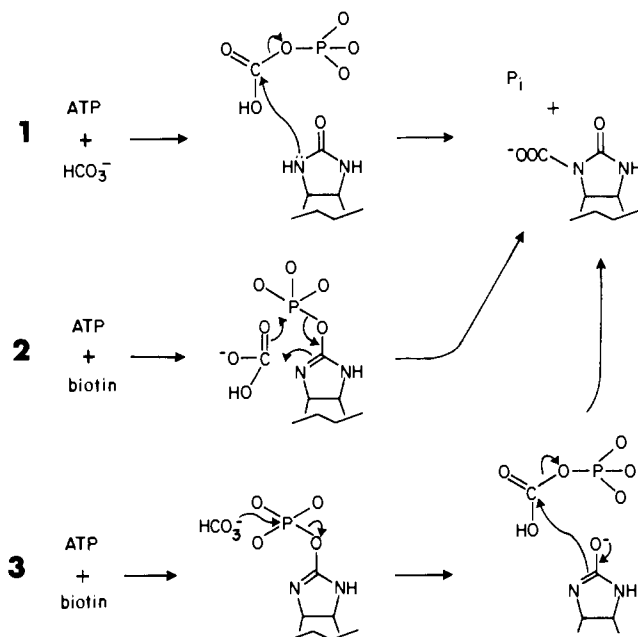


Figure 1. Three postulated mechanisms for the formation of  $N_1$ -carboxybiotin.

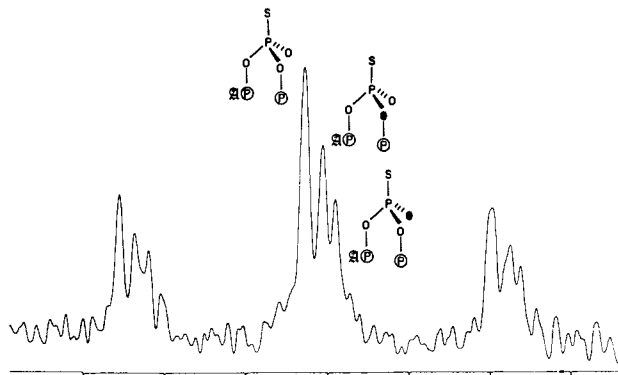


Figure 2.  $^{31}P$  NMR spectrum of the  $\beta$ -phosphorus of ATP $\beta$ S derived from the stereochemical analysis of the inorganic [ $^{16}O$ ,  $^{17}O$ ,  $^{18}O$ ]thiophosphate obtained in the pyruvate carboxylase reaction. The spectrum was obtained on a Bruker WM-300 instrument at 121.5 MHz with a deuterium field lock and broad-band decoupling: spectral width 600.24 Hz; acquisition time 13.65 s; pulse width 24.5 s; number of transients 3000; Gaussian multiplication with Gaussian broadening, 0.016 Hz, and line broadening, -0.300 Hz. The chemical shifts for the nine major resonances:<sup>24</sup> 29.9544, 29.9353, 29.9179, 29.7259, 29.7039, 29.6887, 29.4983, 29.4744, 29.4617 ppm; downfield from external 85% phosphoric acid. Scale: 0.10 ppm per division. The  $\alpha$ - and  $\gamma$ -phospho groups of ATP $\beta$ S are abbreviated by  $\theta$ , adenosine by  $\alpha$ , and  $^{18}O$  by  $\bullet$ .

to form the products. In mechanism 2 ("concerted"), ATP is first attacked by the ureido oxygen atom of biotin<sup>5</sup> to give  $O$ -phosphobiotin, which then undergoes a chemically unprecedented six-electron electrocyclic process with bicarbonate. In mechanism 3 ("composite"),  $O$ -phosphobiotin is formed as above but is attacked by bicarbonate to form carboxy phosphate and the enolic form of biotin (in which the  $N_1$  nitrogen is now nucleophilic<sup>6</sup>), and these two intermediates then react to give the products. This third mechanism is supported by chemical precedent and is analogous to the preferred pathway for the enzyme phosphoenolpyruvate carboxylase.<sup>7</sup>

To narrow the mechanistic possibilities, we have determined the stereochemical fate of the terminal phospho group of adenosine

(1) Kaziro, Y.; Hass, L. F.; Boyer, P. D.; Ochoa, S. *J. Biol. Chem.* **1962**, *237*, 1460.

(2) Wood, H. G.; Barden, R. E. *Annu. Rev. Biochem.* **1977**, *46*, 385. Biotin is normally covalently attached to an enzyme by an amide linkage to a lysyl residue.

(3) Attwood, P. V.; Keech, D. B. *Curr. Top. Cell. Regul.* **1984**, *23*, 1; Kluger, R.; Davis, P. P.; Adawadkar, P. D. *J. Am. Chem. Soc.* **1979**, *101*, 5995.

(4) Caplow, M. *J. Am. Chem. Soc.* **1965**, *87*, 5774.

(5) Bruce, T. C.; Hegarty, A. F. *Proc. Natl. Acad. Sci. U.S.A.* **1970**, *65*, 805.

(6) Hegarty, A. F.; Bruce, T. C.; Benkovic, S. J. *J. Chem. Soc. Chem. Commun.* **1969**, 1173.

(7) Hansen, D. E.; Knowles, J. R. *J. Biol. Chem.* **1982**, *257*, 14795.